厚生労働科学研究費補助金（医療機器開発推進研究事業）
分担研究報告書

アミロスフェロイドの分子構造解析による神経毒性の発現機構解析に関する研究

研究分担者　　廣明　秀一　神戸大学大学院医学研究科特命教授

研究要旨
アルツハイマー病などの認知症は、高齢化している我が国が、率先して取り組むべき課題である。研究代表者らが発見した、極めて強い神経毒性を持つ球状のAβ集合体＝アミロスフェロイドのユニークな分子構造を解明し、その神経細胞死機構と形成機序を解明することは、現状では未解明のシナプス変性以降のアルツハイマー病発症の過程を明らかにし、より有効な治療法開発を可能にすると期待される。我々は、ＮＭＲを中心に、アミロスフェロイドの構造、特に神経細胞と相互作用する部位を解析し、構造情報に基づく分子標的薬剤並びにナノセンサ分子の開発にアプローチすることを計画した。ＮＭＲでペプチドおよびペプチド重合体などの高分子を解析するために$^{13}C/^{15}N$などの安定同位体標識を施す必要がある。我々は、マルトース結合タンパク質-TEVプロテアーゼ切断サイト-Aβ(1-40)/(1-42)　の融合タンパク質を大腸菌で発現する系を作成し、$^{13}C/^{15}N$をが唯一の炭素・窒素源とする培地で培養することで、それらの安定同位体標識を施したアミロイドペプチドを調製した。Aβ(1-40)に関して、^{15}N標識を施した試料を大腸菌から組換え蛋白質として生産することができた。^{15}N-Aβ(1-40)の単量体のNMRスペクトルの測定を行った。^{15}N-Aβ(1-40)から作成したアミロスフェロイドのNMR測定に成功し、一部のシグナルが観測できた。

Ａ．研究目的

アルツハイマー病などの認知症は、高齢化している我が国が、率先して取り組むべき課題である。その治療のためには、本研究が目的とする、シナプス変性以降に起きる神経細胞死の分子機構のヒト脳における解明が必要である。研究代表者らが発見した、極めて強い神経毒性を持つ球状のAβ集合体＝アミロスフェロイドのユニークな分子構造を解明し、その神経細胞死機構と形成機序を解明することは、現状では未解明のシナプス変性以降のアルツハイマー病発症の過程を明らかにし、より有効な治療法開発を可能にすると期待される。そこで、研究代表者の総括の下、ＮＭＲを中心に、Ｘ線結晶構造解析、極低温電子顕微鏡法を用いてアミロスフェロイドの構造、特に神経細胞と相互作用する部位を解析し、構造情報に基づく分子標的薬剤並びにナノセンサ分子の開発にアプローチすることが計画された。そのうち、当研究分担班においては、（１）アミロスフェロイドのＮＭＲ測定を行いそのユニークな構造を解明するための物性データを取得する、（２）そのために種々の安定同位体標識を施したアミロスフェロイドを大量に合成する系を確立する、ことを目的として研究を進めた。

Ｂ．研究方法

ＮＭＲでペプチドおよびペプチド重合体などの高分子を解析するためには、^{1}Hのみの情報ではシグナルが高度に重なるため信号の帰属・解析が困難となるので、通常は$^{13}C/^{15}N$などの安定同位体標識を施すのが一般的である。Aβ(1-40)に安定同位体標識を施すには、安定同位体を含有するアミノ酸を原料とした化学合成ではコストが高くつきすぎ、一般的ではない。そこで我々は、マルトース結合タンパク質-TEVプロテアーゼ切断サイト-Aβ(1-40)/(1-42)　の融合タンパク質を大腸菌で発現する系を作成し、$^{13}C/^{15}N$をが唯一の炭素・窒素源とする培地で培養することで、それらの安定同位体標識を施したアミロイドペプチドを調製することを試みた。まず^{15}N-Aβ(1-40)を得ることを目指して、培養条件・精製条件の検討を行った。得られた試料を確認するためNMR測定を行った。また得られた試料からアミロスフェロイドを試作し、NMRスペクトルの比較を試みた。

（倫理面への配慮）

本研究はヒトに対する研究を含まず、倫理面への配慮には該当しない。遺伝子組換え実験については、カルタヘナ法ならびに神戸大学の基準を順守して管理区域内で行った。

C．研究結果

1. Aβ(1-40)に関して、^{15}N標識を施した試料を大腸菌から組換え蛋白質として生産することができた。
2. ^{15}N-Aβ(1-40)の単量体のNMRスペクトルの測定を行った。
3. ^{15}N-Aβ(1-40)の一部をアミロスフェロイドとすることができた。ただし収率は低く、今後の改善が必要であった。
4. ^{15}N-Aβ(1-40)から作成したアミロスフェロイドのNMR測定に成功し、一部のシグナルが観測できた。

D．考察

^{15}N-Aβ(1-40)から作成したアミロスフェロイドのNMR測定に成功し、一部のシグナルが観測できたことから、その分子の対称性などについて一定の知見が得られた。すなわち、Aβ(1-40)のN末端およそ10残基と、分子中央の一部分はアミロスフェロイド球状構造から露出し、分子表面でフレキシブルな構造をとっていると考えられる。また、この部分が、受容体と作用してアミロスフェロイドの高毒性を発揮すると考えられた。

^{15}N標識アミロスフェロイドから得られる情報を相補するために、今後は^{13}C標識を施したAβ(1-40)由来またはAβ(1-42)由来アミロスフェロイドを順次調製し、NMR観測を行う。

今回の研究により、大腸菌発現系由来のAβ(1-40)は、含まれている夾雑物などの特性が化学合成ペプチドのそれとは大きく異なるため、アミロスフェロイド化の重合反応は予定していたよりも低いことがわかった。今後、このステップの条件検討が必要である。また、生理学的に重要でアミロスフェロイド収率も良好な、Aβ(1-42)をプロトマーとしたアミロスフェロイドの調製を行う必要がある。

E．結論

^{15}N-Aβ(1-40)からアミロスフェロイドを一部含むと思われる重合体が作成でき、そのNMR測定に成功し、一部のシグナルが観測できた。

F．健康危険情報

総括研究報告書を参照

G．研究発表

1. 論文発表

その他　書籍

廣明秀一：NMRの原理　核磁気共鳴分光法　（分光測定入門シリーズ８）p1-32，日本分光学会編、講談社サイエンティフィク(2009)

2. 学会発表

1. 廣明秀一，　P.horikoshiiのStomatinPH0470のSPFHドメインオリゴマーの特異な熱解離，JST-CNRS合同「マリーンゲノム・バイオ分野」セミナー新規ウイルス様膜小胞体の発見と超好熱性古細菌での機能解明に向けて，筑波研究支援センター，筑波，2009/10/30，招待講演
2. 合田（天野）名都子，　清水佳奈，桑原陽太，野口保，池上貴久，太田元規，廣明秀一，　NMRによる天然変性タンパク質配列の網羅的検証法，日本生物物理学会第47回年会，アスティとくしま，徳島，2009/10/30-11/1，一般講演
3. 廣明秀一，　基礎から理解する溶液NMRの最新技術，第48回NMR討論会-チュートリアルコース，九州大学馬出病院キャンパスコラボステーションI，福岡，2009/11/9，招待講演
4. 廣明秀一，　NMRの原理，分光学会第45回夏期セミナー，幕張メッセ国際会議場，東京，2009/9/3，招待講演
5. 桑原陽太，　雲財悟，永田崇，池上貴久，廣明洋子，藤吉好則，廣明秀一，　熱により不可逆的に解離するPH0470由来のSPFHドメイン多量体，第９回日本蛋白質科学会年会，熊本全日空ホテルニュースカイ，熊本，2009/5/20-22，ポスター
6. 天野剛志，合田（天野）名都子，廣明秀一，LBT/PTD-Dual-Tag蛋白質発現ベクターの開発とPTD配列の細胞内取り込み機構の解析，ＣＲＥＳＴ「生命現象」平成２１年度中間報告会・終了報告会，千里ライフサイエンスセンター，大阪，2009/11/24-25，ポスター
7. 藤原芳江，　合田（天野）名都子，　岩谷奈央子，　白川昌宏，廣明秀一，　Innovative Nanoscience of Supermolecular Motor Proteins Working in Biomembranes，京都大学芝蘭会館，京都，2009/9/8-10，ポスター
8. 藤原芳江，　岩谷奈央子，　藤原健一朗，白川昌宏，廣明秀一，　核に存在するVCP様タンパク質，NVL2のN末端ドメインの解析，第56回日本生化学会近畿支部例会，大阪医科大学，大阪，2009/7/11，一般講演
9. 藤原芳江，　岩谷奈央子，　藤原健一朗，白川昌宏，廣明秀一，　核に存在するVCP様蛋白質NVL2のN末端ドメインの解析，第９回日本蛋白質科学会年会，，熊本全日空ホテルニュースカイ，熊本，

2009/5/20-22, ポスター
10. 藤原芳江, 藤原健一朗, 合田（天野）名都子, 岩谷奈央子, 天野剛志, 白川昌宏, 廣明秀一, 核に存在するVCP様蛋白質, NVL2のN末端ドメインの構造・機能解析, 第２回神戸大学バイオサイエンス・若手研究者交流会, 兵庫, 2010/2, ポスター
11. 合田（天野）名都子, 清水佳奈, 桑原陽太, 天野剛志, 池上貴久, 太田元規, 廣明秀一, PRESAT-vectorを用いた天然変性タンパク質配列の網羅的検証系の確立, 第32回日本分子生物学会年会, パシフィコ横浜, 横浜, 2009/12/9-12, ポスター
12. 廣明秀一, ドメイン構造から理解するＡＡＡ-ＡＴＰａｓｅの機能分担, 京都大学低温物質科学研究センター第8回講演会・研究交流会「構造生物学の現状と未来」, 京都大学百年記念講堂, 京都, 2010/3/15, 招待講演

H. 知的財産権の出願・登録状況
（予定を含む。）
なし

厚生労働科学研究費補助金（医療機器開発推進研究事業）
分担研究報告書

ウィルスベクターを用いたアミロスフェロイドの機能解析に関する研究

研究分担者　村松慎一　自治医科大学・内科学講座神経内科学部門　特命教授

研究要旨
認知症（痴呆症）の主要な原因であるアルツハイマー病の発症には，球状のAβアミロイド蛋白(アミロスフェロイド)が関与していると推察される．アミロスフェロイドの病態生理学的意義を明らかにし，アルツハイマー病の早期診断と治療法を開発することを目標として研究を行った．アミロスフェロイドの生体内における病態を解析するために，実験動物の脳内で神経細胞特異的にAβ蛋白を発現することにより持続してアミロスフェロイドを供給できると考えられるアデノ随伴ウイルス（AAV）ベクターを作製し，定位脳手術によりマウスおよびカニクサルの海馬に投与した．AAVベクターには神経細胞特異的プロモーターを使用し，Sweden型変異を持つアミロイド前駆体蛋白質を発現させた．

A．研究目的

アルツハイマー病は，近年の高齢化人口の増加に伴い重要な社会問題となっている認知症（痴呆症）の主要な原因である．アルツハイマー病では，脳内にAβアミロイド蛋白の蓄積が認められ，Aβが神経細胞死を引き起こすと考えられている．Aβの神経毒性の機序を解明することは，アルツハイマー病の発症予防および治療法の開発のために重要である．

本研究では，Aβが球状の構造（アミロスフェロイド）をとることにより毒性を発揮するという星らの仮説を霊長類のモデルにより検証し新たな治療法を開発することを目的としている．

B．研究方法

（1）AAVベクターの作製

CAGプロモーターあるいは神経細胞特異的Synapsine I (Syn I)プロモーターの下流にアミロイド前駆体蛋白(APP)のcDNAを繋ぎ,SV40 poly(A)配列とともに 3型AAVのinverted terminal repeats (ITR)配列の間に挿入した．8型AAVのカプシドを発現するプラスミドとともに293細胞にトランスフェクションし，CsClの密度勾配により組換えAAVベクターを作製した．APP蛋白は野生型の他に，家族性アルツハイマー病におけるSweden型変異APP($Lys^{670}\rightarrow Asn^{670}$, $Met^{671}\rightarrow Leu^{671}$)についてもAAVベクターを作製した．

（2）マウス・サル脳内へのAPP遺伝子導入

(1)で作製したAAVベクターを定位脳手術により，C57BL6マウスとカニクイサルの海馬に注入した.カニクイサルの定位脳手術に際しては，MRI画像を使用したナビゲーションシステムを応用した．

C．研究結果

（1）マウス海馬へのAAV-APP注入

SynIプロモーターにより野生型,およびSweden型変異APPをそれぞれ発現するAAVを海馬に注入したマウスでは，注入12か月までの時点で明らかな行動変化は見られていない．今後，引き続き観察を継続するとともに，認知機能についての行動解析を行う．

（2）サル脳内でのAPPの発現

SynIプロモーターによりAPPを発現するAAVを海馬と大脳皮質に注入した２頭の若年サルでは，6か月後の組織解析では，明らかな細胞脱落は認められなかった．CAGプロモーターを搭載したAAVベクターを海馬に注入した老齢サルについては，注入直後のMRIにより，海馬の広範な領域にベクターが拡散していることが確認できた．現在，ベクター投与18か月後に安楽殺したカニクイサルの脳組織について解析中である．

（倫理面での配慮）

動物個体での実験手法は，法律第105 号「動物の愛護及び管理に関する法律」，総理府「実験動物の飼養及び保管に関する基準」，文部省通知「大学等における動物実験について」，日本霊長類学会「サル類を用いる実験遂行のための基本原則」を遵守し，自治医大の動物実験委員会の承認を得て行った．

D．考察

これまでの研究で，カニクイサルの脳内へのアミロスフェロイドの単回注入では，明らかな毒性は認められなかった．培養細胞と異なり，脳内では手術操作による一時的な炎症とそれによるアミロスフェロイド除去反応が生じる可能性などが考えられるため，持続してアミロスフェロイドを作用させることが望ましい．そのため，アデノ随伴ウイルス（AAV）ベクターによりAPPを発現させる方法を開発した．AAVベクターは脳内の神経細胞に効率よく遺伝子を導入し，炎症・免疫反応をほとんど惹起することなく長期発現させることが可能である．

2型あるいは3型AAVベクターを使用すれば神経細胞にほぼ選択的に遺伝子導入できるが，SynIプロモーターを使用することで神経細胞特異的にAPPを発現できる．若年サル大脳皮質および海馬への注入では，明らかな神経細胞死は見いだせなかったが，若年サルでは，アミロイド分解酵素であるネプリライシンの活性が高いなど，種々の解毒作用が働いている可能性がある．今後，老齢サルの脳組織を詳細に解析することにより，神経細胞死の誘導とアミロスフェロイドが毒性を発揮する局面を捕捉できるものと考えられる．

E. 結論

アルツハイマー病におけるアミロスフェロイドの神経細胞に対する毒性の発現機構の解明を目標として研究を行った．APPを発現するAAVベクターを作製し，マウスとカニクサルの脳内に投与した．次年度も解析を継続する．

F. 健康危険情報

総括研究報告書を参照

G.研究発表

1.論文発表

E. Fukushima F, Nakao K, Shinoe T, Fukaya M, Muramatsu S, Sakimura K, Kataoka H, Mori H, Watanabe M, Manabe M, Mishima M : Ablation of NMDA receptors enhances the excitability of hippocampal CA3 neurons. PLoS ONE, 4(1):e3993, 2009.

F. Kuratomi S, Ohmori Y, Ito M, Shimazaki K, Muramatsu S, Mizukami H, Uosaki H, Yamashita JK, Arai Y, Kuwahara K, Takano M : The cardiac pacemaker-specific channel Hcn4 is a direct transcriptional target of MEF2. Cardiovasc Res, 83(4):682-687, 2009.

G. Muramatsu, S, Okuno T, Suzuki Y, Nakayama T, Kakiuchi T, Takino N, Iida A, Ono F, Terao K, Inoue N, Nakano I, Kondo Y and Tsukada H: Multi-tracer assessment of dopamine function after transplantation of embryonic stem cell-derived neural stem cells in a primate model of Parkinson's disease. Synapse, 63:541-548, 2009.

H. Tanaka Y, Ikeda T, Masuda S, Shibata H, Takeuchi K, Komura M, Iwanaka T, Muramatsu S, Kondo Y, Takahashi K, Yamanaka S and Hanazono Y : ERas is expressed in primate embryonic stem cells but not related to tumorigenesis. Cell Transplant, 18(4):381-389, 2009.

I. Okuno T, Nakayama T, Konishi N, Michibata H, Wakimoto K, Suzuki Y, Nito S, Inaba T, Nakano I, Muramatsu S, Takano M, Kondo Y, Inoue N: Self-contained induction of neurons from human embryonic stem cells. PLoS ONE, 4:e6318, 2009.

J. Ito T, Yamamoto S, Hayashi T, Kodera M, Mizukami H, Ozawa K, Muramatsu S: A convenient enzyme-linked immunosorbent assay for rapid screening of anti-adeno-associated virus neutralising antibodies. Ann Clin Biochem, 46(Pt 6):508-510, 2009.

K. Noguchi, A, Matsumura, S, Dezawa, M, Tada, M, Yanazawa, M, Ito, A, Akioka, M, Kikuchi, S, Sto, M, Ideno, S, Noda, M, Fukunari, A, Muramatsu, S, Itokazu, Y, Sato, K, Takahashi, H, Teplow, DB, Nabeshima, Y, Kakita, A, Imahori, K, Hoshi, M: Isolation and characterization of patient-derived, toxic, high-mass amyloid b-protein (Ab) assembly from Alzheimer's disease brains. J Biol Chem, 284(47):32895-905, 2009.

L. Kadkhodaei, B, Ito, T, Joodmardi, E, Mattsson, B, Rouillard, C, Carta, M, Muramatsu, S, Ichinose, C, Nomura, T, Chambon, P, Metzger, D, Larsson, N, Lindqvist, E, Olson, L, Bjorklund, A, Ichinose, H: Nurr1 is Required for Maintenance of Maturing and Adult Midbrain Dopamine Neurons. J Neurosci, 29(50):15923-15932,2009.

2. 学会発表

1. 村松慎一：パーキンソン病の再生医学．第50回日本神経学会総会，仙台，2009年5月22日．(プログラム p45)

2. 浅利さやか，村松慎一：パーキンソン病の遺伝子治療のPET解析．第50回日本神経学会総会，仙台，2009年5月22日．(プログラム p121)

3. Muramatsu S, Fujimoto K, Kato S, Asari S, Mizukami H, Ikeguchi K, Kawakami T, Urabe M, Kume A, Sato T, Watanabe E, Ozawa K and Nakano I: "Aromatic L-amino acid decarboxylase gene therapy for Parkinson's disease: results from an open-label, phase I trial" , The American

society of gene therapy (ASGT)' s 12th annual meeting, San Diego, May 29, 2009.

4. 伊藤哲男, 林司, 古寺美加, 水上浩明, 小澤敬也, 三室淳, 坂田洋一, 村松慎一: 中和抗体法と相関性のある抗 AAV2 抗体検出試薬の開発. 第 32 回日本血栓止血学会学術集会, 北九州, 2009 年 6 月 5 日. (日本血栓止血学会誌 20(2), p204)
5. Muramatsu S, Fujimoto K, Kato S, Asari S, Mizukami H, Ikeguchi K, Kawakami T, Urabe M, Kume A, Sato T, Watanabe E, Ozawa K and Nakano I : Phase I trial of AAV vector-mediated gene delivery of aromatic L-amino acid decarboxylase for parkinson' s disease. The Japan society of gene therapy' s 15th annual meeting. Osaka, July 11, 2009.
6. 村松慎一, 一瀬宏 : 線条体のドパミン代謝 : 新たな視点と治療. 第 32 回日本神経科学大会, 名古屋, 2009 年 9 月 17 日. (プログラム p84)

H. 知的財産権の出願・登録状況

なし

研究成果の刊行に関する一覧表

雑誌

発表者氏名	論文タイトル名	発表誌名	巻号	ページ	出版年
Roychaudhuri, R., Yang, M., Hoshi, M.M., and Teplow, D.B.	**Amyloid β-protein assembly and Alzheimer disease**	*J. Biol. Chem.*	284	4749-4753	2009
Noguchi, A., Matsumura, S., Dezawa, M., Tada, M., Yanazawa, M., Ito, A., Akioka, M., Kikuchi, S., Sato, M., Ideno, S., Noda, M., Fukunari, A., Muramatsu, S., Itokazu, Y., Sato, K., Takahashi, H., Teplow, D.B., Nabeshima, Y., Kakita, A., Imahori, K., and *Hoshi, M.	**Isolation and characterization of patient-derived, toxic, high-mass amyloid β-protein (Aβ) assembly from Alzhiemer's disease brains**	*J. Biol. Chem.*	284	32895-32905	2009
Kitamura, Y., Yanazawa, M., Sato, M., Ito, A., and Hoshi, M.M.	**Identification of amylospheroid-b proteins from mature neurons as molecular target of neurotoxicity by nonfibrillar Aβ assemblies**	**Alzheimer's and Dementia**	5	222-223	2009
K. Noma, K. Kimura, K. Minatohara, H. Nakashima, Y. Nagao, A. Mizoguchi and Y. Fujiyoshi	Triple *N*-Glycosylation in the Long S5-P Loop Regulates the Activation and Trafficking of the Kv12.2 Potassium Channel	***J. Biol. Chem***	284	33139-33150	2009
A. Inutsuka, M. Goda and Y. Fujiyoshi	Calyculin A-induced neurite retraction is critically dependent on actomyosin activation but not on polymerization state of microtubules	***Biochem. Biophys. Res. Commun***	390	1160-1166	2009
K. Abe, K. Tani and Y. Fujiyoshi	Structural and functional characterization of H^+,K^+- ATPase with bound fluorinated phosphate analogs	***J. Struct. Biol***	170	60-68	2010
K. Irie, K. Kitagawa, H. Nagura, T, Imai, T. Shimomura and Y. Fujiyoshi	Comparative study of the gating motif and C-type inactivation in prokaryotic voltage-gated sodium channels.	***J. Biol. Chem***	285	3685-3694	2010
Mizukami, S., Watanabe, S., Hori, Y., Kikuchi, K.	Covalent protein labeling based on noncatalytic β-lactamase and a designed FRET substrate.	*J. Am. Chem. Soc.*	131	5016-5017	2009

Mizukami, S., Takikawa, R., Sugihara, F., Shirakawa, M., Kikuchi, K.	Dual-function probe to detectprotease activity for fluorescence measurement and ^{19}F MRI.	*Angew. Chem. Int. Ed.*	48	3641-3543	2009
Mizukami, S., Watanabe, S., Kikuchi, K.	Development of ratiometric fluorescent probes for phosphatases by using a pK_a switching mechanism.	*Chembiochem*	48	1465-1468	2009
Yamaguchi, S., Miura, C., Kikuchi, K., Celino, F. T., Agusa, T., Tanabe, S., Miura, T.	Zinc is an Essential Trace Element for Spermatogenesis.	*Proc. Natl. Acad. Sci. U. S. A.*	106	10859-10864	2009
Kikuchi, K., Hashimoto, S., Mizukami, S., Nagano, T.	Anion sensor-based ratiometric peptide probe for protein kinase activity.	*Org. Lett.*	11	2732-2735	2009
Mizukami, S., Okada, S., Kimura, S., Kikuchi, K.	Design and synthesis of coumarin-based Zn^{2+} probes for ratiometric fluorescence imaging.	*Inorg. Chem.*	48	7630-7638	2009
Hori, Y., Ueno, H., Mizukami, S., Kikuchi, K.	Photoactive yellow protein-based protein labeling systemwith turn-on fluorescence intensity.	*J. Am. Chem. Soc.*	131	16610-16111	2009
Hori, Y., Egashira, Y., Kamiura, R., Kikuchi, K.	Noncovalent-Interaction-Promoted Ligation for Protein Labeling.	*Chembiochem*	11	646-648	2010
Fukushima F, Nakao K, Shinoe T, Fukaya M, Muramatsu S, Sakimura K, Kataoka H, Mori H, Watanabe M, Manabe M and Mishima M	Ablation of NMDA receptors enhances the excitability of hippocampal CA3 neurons.	PLoS ONE	4(1)	e3993	2009
Kuratomi S, Ohmori Y, Ito M, Shimazaki K, Muramatsu S, Mizukami H, Uosaki H, Yamashita JK, Arai Y, Kuwahara K and Takano M	The cardiac pacemaker-specific channel Hcn4 is a direct transcriptional target of MEF2.	Cardiovasc Res	83(4)	682-687	2009
Muramatsu S, Okuno T, Suzuki Y, Nakayama T,	Multi-tracer assessment of dopamine function after transplantation of embryonic stem	Synapse	63	541-548	2009

Kakiuchi T, Takino N, Iida A, Ono F, Terao K, Inoue N, Nakano I, Kondo Y and Tsukada H	cell-derived neural stem cells in a primate model of Parkinson's disease.				
Tanaka Y, Ikeda T, Masuda S, Shibata H, Takeuchi K, Komura M, Iwanaka T, Muramatsu S, Kondo Y, Takahashi K, Yamanaka S and Hanazono Y	ERas is expressed in primate embryonic stem cells but not related to tumorigenesis.	Cell Transplant	18(4)	381-389	2009
Okuno T, Nakayama T, Konishi N, Michibata H, Wakimoto K, Suzuki Y, Nito S, Inaba T, Nakano I, Muramatsu S, Takano M, Kondo Y, and Inoue N	Self-contained induction of neurons from human embryoniv stem cells.	PLoS ONE	4	e6318	2009
Ito T, Yamamoto S, Hayashi T, Kodera M, Mizukami H, Ozawa K and Muramatsu S	A convenient enzyme-linked immunosorbent assay for rapid screening of anti-adeno-associated virus neutralising antibodies.	Ann Clin Biochem	46(Pt 6)	508-510	2009
Kadkhodaei B, Ito T, Joodmardi E, Mattsson B, Rouillard C, Carta M, Muramatsu S, Ichinose C, Nomura T, Chambon P, Metzger D, Larsson N, Lindqvist E, Olson L, Bjorklund A and Ichinose H	Nurr1 is required for maintenance of maturing and adult midbrain dopamine neurons.	J Neurosci	29(50)	15923-15932	2009
廣明秀一	NMRの原理 核磁気共鳴分光法	分光測定入門シリーズ８ 日本分光学会編、講談社サイエンティフィク		1-32	2009

IV. 研究成果の刊行物・別刷り

THE JOURNAL OF BIOLOGICAL CHEMISTRY VOL. 284, NO. 47, pp. 32895–32905, November 20, 2009

Isolation and Characterization of Patient-derived, Toxic, High Mass Amyloid β-Protein (Aβ) Assembly from Alzheimer Disease Brains*[S]

Received for publication, March 2, 2009, and in revised form, September 10, 2009 Published, JBC Papers in Press, September 15, 2009, DOI 10.1074/jbc.M109.000208

Akihiko Noguchi,[a] Satoko Matsumura,[a] Mari Dezawa,[b,c] Mari Tada,[d] Masako Yanazawa,[a] Akane Ito,[a] Manami Akioka,[a] Satoru Kikuchi,[a] Michio Sato,[a] Shouji Ideno,[e] Munehiro Noda,[e] Atsushi Fukunari,[e] Shin-ichi Muramatsu,[f] Yutaka Itokazu,[b] Kazuki Sato,[g] Hitoshi Takahashi,[d] David B. Teplow,[h] Yo-ichi Nabeshima,[b] Akiyoshi Kakita,[d] Kazutomo Imahori,[i] and Minako Hoshi[a,b1]

From the [a]Mitsubishi Kagaku Institute of Life Sciences, Tokyo 194-8511, Japan, [b]Kyoto University, Kyoto 606-8501, Japan, [c]Tohoku University, Sendai 908-8575, Japan, [d]Niigata University, Niigata 951-8585, Japan, [e]Mitsubishi Tanabe Pharma Corporation, Osaka 541-8505, Japan, [f]Jichi Medical University, Tochigi 329-0498, Japan, [g]Fukuoka Women's University, Fukuoka 813-8529, Japan, the [h]David Geffen School of Medicine, UCLA, Los Angeles, California 90095, and [i]University of Tokyo, Tokyo 113-8654, Japan

Amyloid β-protein (Aβ) assemblies are thought to play primary roles in Alzheimer disease (AD). They are considered to acquire surface tertiary structures, not present in physiologic monomers, that are responsible for exerting toxicity, probably through abnormal interactions with their target(s). Therefore, Aβ assemblies having distinct surface tertiary structures should cause neurotoxicity through distinct mechanisms. Aiming to clarify the molecular basis of neuronal loss, which is a central phenotype in neurodegenerative diseases such as AD, we report here the selective immunoisolation of neurotoxic 10–15-nm spherical Aβ assemblies termed native amylospheroids (native ASPDs) from AD and dementia with Lewy bodies brains, using ASPD tertiary structure-dependent antibodies. In AD patients, the amount of native ASPDs was correlated with the pathologic severity of disease. Native ASPDs are anti-pan oligomer A11 antibody-negative, high mass (>100 kDa) assemblies that induce degeneration particularly of mature neurons, including those of human origin, *in vitro*. Importantly, their immunospecificity strongly suggests that native ASPDs have a distinct surface tertiary structure from other reported assemblies such as dimers, Aβ-derived diffusible ligands, and A11-positive assemblies. Only ASPD tertiary structure-dependent antibodies could block ASPD-induced neurodegeneration. ASPDs bind presynaptic target(s) on mature neurons and have a mode of toxicity different from those of other assemblies, which have been reported to exert their toxicity through binding postsynaptic targets and probably perturbing glutamatergic synaptic transmission. Thus, our findings indicate that native ASPDs with a distinct toxic surface induce neuronal loss through a different mechanism from other Aβ assemblies.

Neurodegenerative diseases, such as Alzheimer disease (AD),[2] Parkinson disease, prion diseases, and the polyglutamine diseases, arise from abnormal protein interactions in the central nervous system (1). In these diseases, complex multistep processes of protein conformational change and accretion produce various nonfibrillar assemblies, leading finally to fibrils (1–5). Recent studies have suggested that the early assemblies in this process might be the most toxic, possibly through the exposure of buried moieties and the formation of surface tertiary structures not present in physiologic monomers (6). These surface tertiary structures could mediate abnormal interactions with other cellular components (1).

In AD, extensive studies have suggested that accumulation of amyloid β-protein (Aβ), a physiologic derivative of amyloid precursor protein (APP), plays a primary pathogenic role (7–9). Various forms of assemblies ranging in mass from dimers up to multimers of ~1 MDa have been reported as neurotoxins (10–13) as follows: protofibrils (14); dimers/trimers (natural low-*n* oligomers) (15); 3–24-mer Aβ-(1–42) assemblies termed Aβ-derived diffusible ligands (ADDLs) (16); 12-mers termed globulomers (17) or Aβ*56 (18); 15–20-mer Aβ assemblies termed Aβ oligomers (AβOs) (19); and 150-mer or higher assemblies termed β-sheet intermediates (20). Whether or not they share a common surface, the tertiary structure responsible

* This work was supported in part, by National Institutes of Health Grant NS038328 (to D. B. T.), by Health and Labour Sciences Research Grants "Research on Nanotechnical Medical" (to M. H.) and "Research on Psychiatric and Neurological Diseases and Mental Health" (to M. D.) from the Ministry of Health, Labor, and Welfare, by Special Coordination Funds for Promoting Science and Technology (to M. H.) from the Ministry of Education, Culture, Sports, Science, and Technology, and by the Program for Promotion of Fundamental Studies in Health Sciences (to M. D.) from the National Institute of Biomedical Innovation The authors declare the following conflict of interest: this work was supported in part by a grant (to M. H.) from Mitsubishi Kagaku Institute of Life Sciences, which is a nonprofit organization financially supported by Mitsubishi Chemical Corp.; this grant expires in March 2009.

[S] The on-line version of this article (available at http://www.jbc.org) contains supplemental Experimental Procedures, Tables S1 and S2, Figs. S1–S7, and additional references.

[1] To whom correspondence should be addressed: Sakyo-ku, Kyoto 606-8501, Japan. E-mail: minhoshi@lmls.med.kyoto-u.ac.jp.

[2] The abbreviations used are: AD, Alzheimer disease; Aβ, amyloid β-protein; APP, amyloid precursor protein; sAPPα, human secreted form of APP; ADDL, Aβ-derived diffusible ligand; AβO, Aβ oligomer; ASPD, amylospheroid; DLB, dementia with Lewy bodies; MALDI-TOF/MS, matrix-assisted laser desorption/ionization time-of-flight mass spectrometry; HFIP, 1,1,1,3,3,3-hexafluoro-2-propanol; PBS, Dulbecco's phosphate-buffered saline without Ca^{2+} and Mg^{2+}; TEM, transmission electron microscopy; IP, immunoprecipitation; NCI, noncognitively impaired; MSCs, bone marrow stromal cells; NMDA-R, *N*-methyl-D-aspartate-type glutamate receptor; DIV, days *in vitro*; NCI, noncognitively impaired.

for toxicity remains unsettled; some of these assemblies are detected by specific antibodies (17, 21), whereas others are detected by a polyclonal A11 antibody (18, 19) that is reported to recognize epitopes associated with a certain oligomer state of amyloids regardless of their amino acid sequence (22). However, these assemblies, which differ in origin, mass, and toxic activity, mostly bind to postsynapses, leading to synaptic impairment (17–19, 23, 24). They are also suggested to play a role in synaptic impairment in AD model mice carrying human APP (17, 18, 25), which retain early features of AD such as amyloid plaques, synaptic loss, and mild memory deficits (26, 27). These observations collectively suggest that these assemblies play a role in AD pathogenesis by causing synaptic impairment. On the other hand, it remains largely unknown how, after the synaptic impairment, these assemblies cause subsequent neuronal loss in human AD brains. One reason is that no overt neuronal cell loss has been observed in most APP transgenic mice (except APP23 mice (28, 29)), even in the presence of these assemblies (26, 27). Another reason is that, as for the nonfibrillar Aβ assemblies actually present in human AD brains, Aβ dimers that induce synaptic impairment and not neuronal loss were recently isolated (30), but Aβ assemblies that directly cause neuronal loss have not yet been isolated either from AD patients or from the mice. Because soluble fractions of brains from humans with AD have been reported to contain Aβ assemblies ranging in size from dimers to polymers larger than 100 kDa (31), which appear to correlate with dementia (32, 33), Aβ assemblies responsible for neuronal loss might be present in the soluble fractions of AD brains. As has recently been shown clinically and diagnostically (34–37), neuronal loss plays an important role in cognitive deterioration of AD patients, so we aimed to isolate toxic Aβ assemblies from the soluble fractions of AD brains.

As a first step to isolate such Aβ assemblies *in vivo*, we have previously prepared highly toxic spherical Aβ assemblies termed "amylospheroids" (ASPDs) *in vitro* (38). Notably, ASPDs are considered not to be intermediates in the pathway leading to fibrils, because ASPDs were not incorporated into mature fibrils and continued to exist after fibril formation (13, 38). They also differ from protofibrils and ADDLs in morphology and size (11, 13, 38).

Here, we generated ASPD tertiary structure-dependent antibodies and used them to selectively immunoisolate a human counterpart of ASPDs (native ASPDs) from patients with AD or dementia with Lewy bodies (DLB). To distinguish native ASPDs from *in vitro*-produced ASPDs, the latter is hereafter referred to as synthetic ASPDs. Native ASPDs are A11-negative, high mass Aβ assemblies that induce degeneration of human neuronal cells *in vitro*, particularly those with mature character, and they differ in mass, surface tertiary structure, and neurotoxicity mechanism from other reported nonfibrillar Aβ assemblies (summary in supplemental Table S1).

EXPERIMENTAL PROCEDURES

Aβ Source—Aβ-(1–40) peptides were synthesized using *N*-(9-fluorenyl)methoxycarbonyl (Fmoc) chemistry on an Applied Biosystems model 433A peptide synthesizer and purified (38). Their structure and purity were confirmed using quantitative amino acid analysis, analytic high pressure liquid chromatography, and matrix-assisted laser desorption/ionization-time-of-flight/mass spectrometry (MALDI-TOF/MS; Ultraflex II, Bruker Daltonics). The purified Aβ-(1–40) was lyophilized, dissolved in 35% (v/v) acetonitrile in 0.1% (v/v) trifluoroacetic acid (~50 nmol/tube), and lyophilized. This step was repeated twice. Aβ-(1–42) peptides (25 mg/ampoule; Bachem lots 0552992 and 1000255) were completely dissolved in ~54 ml of 1,1,1,3,3,3-hexafluoro-2-propanol (Aldrich) by incubating the peptide solution overnight at 4 °C and then for 3 h at 37 °C and finally lyophilized (~40 nmol/tube). This step was repeated two or three times. The lyophilized peptides were kept at −20 °C.

Preparation and Purification of Synthetic ASPDs—Synthetic ASPDs were prepared *in vitro* either from 50 μM solution of Aβ-(1–40) (0.5× Dulbecco's phosphate-buffered saline without Ca^{2+} and Mg^{2+} (PBS); Nissui Pharmaceutical Co. Ltd.) or of Aβ-(1–42) (either 0.5× PBS or F12 buffer without L-glutamine and phenol red) by slowly rotating the solution (5–7 days for Aβ-(1–40); 14 h for Aβ-(1–42)), as described previously (38). At concentrations below a critical fibril-forming concentration (~100 μM) (39), spherical Aβ assemblies (5–20 nm in diameter for Aβ-(1–40); 5–25 nm for Aβ-(1–42); >85% 10–15 nm spheres), with rare fibril-like structures, were usually produced. The most toxic ASPDs (prepared either from Aβ-(1–40) or Aβ-(1–42)) were previously identified as 10–15-nm spheres recovered by glycerol gradient centrifugation in the fraction migrating near the thyroglobulin (669 kDa) standard (38). Further analysis of standard proteins using this glycerol gradient sedimentation assay revealed that the mass of the most toxic ASPDs is approximately equal to that of aldolase (158 kDa) but does not exceed that of thyroglobulin (669 kDa).[3] Therefore, the most toxic ASPDs were purified as retentates by using 100-kDa molecular mass cutoff filters (Ultrafree-MC, Millipore) to remove lower mass Aβ assemblies. In some experiments, including mature neuron-binding assays, the most toxic ASPD fraction was also purified by two-step filtrations (see Scheme 1). Studies using transmission electron microscopy (TEM) revealed that 10–15-nm spheres were predominantly recovered in the most toxic ASPD fraction (termed "158–669-kDa ASPDs") that passed through 0.22-μm filters but were retained on 100-kDa molecular mass cutoff filters (data not shown). Although these 10–15-nm spheres were hardly detectable in 100-kDa filtrates, smaller particles with a diameter of 5–6 nm were present in 100-kDa filtrates. A very small amount of 10–15-nm ASPDs was also present in 0.22-μm retentates because they remained bound to the filter (data not shown). These TEM observations were in good agreement with the results of dot blots and toxicity assays shown in Fig. 1*A*. Quantitative amino acid analysis revealed that generally ~25% of total Aβ was recovered as 158–669-kDa ASPDs. Synthetic ASPDs were prepared every week, and their quality was confirmed using dot blotting, TEM, and toxicity assays. Aβ concentration of each preparation was deter-

[3] A. Noguchi and M. Hoshi, unpublished data.

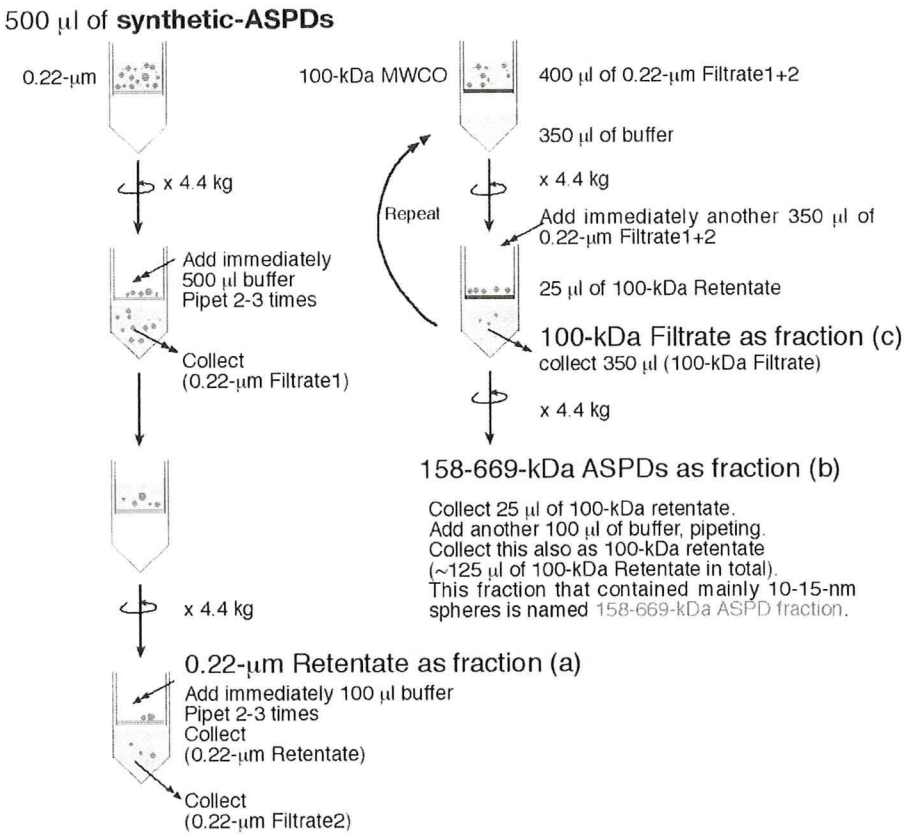

SCHEME 1. **Fractionation of the most toxic 158–669-kDa ASPDs by two-step filtrations.**

mined every week by quantitative amino acid analysis (Waters AccQ-Tag system) (38).

Preparation of Aβ Monomers and Fibrils—To prepare monomers, Aβ-(1–40) or Aβ-(1–42) lyophilizates were solubilized to 50 μM in 1,1,1,3,3,3-hexafluoro-2-propanol. The solution was incubated for 30 min at room temperature and then centrifuged at 20,400 × *g* for 30 min at 4 °C, and the upper 90% of the supernatant volume was collected. The monomer concentration was determined by means of quantitative amino acid analysis (38). To produce fibrils, Aβ-(1–40) was dissolved at a concentration of 100 μM in 0.5× PBS, pH 3.5. This solution was incubated without agitation at 37 °C for 2 days, after which fibrils were separated from the monomer and low mass Aβ assemblies by filtration through 100-kDa molecular mass cutoff filters. Large amounts of fibrils without ASPDs were detected reproducibly by TEM. The fibril concentration was determined by means of quantitative amino acid analysis (38). To obtain different types of fibrils for immuno-TEM analysis, fibrils were also produced by slowly rotating the above Aβ-(1–40) solution or by dissolving Aβ-(1–40) at a concentration of 350 μM in PBS, pH 7.5, followed by incubation for 5–7 days at 37 °C, with or without slow rotation (38).

Preparation of Aβ Oligomers for A11 Antibody—A test membrane, on which soluble Aβ oligomers (termed AβOs) and Aβ fibrils (1–3 μg/dot) were spotted, was produced by Dr. C. Glabe (University of California, Irvine) according to reported methods (22, 40). This test membrane was kindly provided by Invitrogen as a positive control for A11 antibody.

Preparation of ADDLs—ADDLs were produced as described previously (16). Aβ-(1–42) lyophilizates were solubilized to 5 mM in DMSO, diluted to 100 μM with F12, and incubated for 24 h at 4 °C. The solution was centrifuged at 14,000 × *g* for 10 min at 4 °C, and the supernatant was collected. These ADDL preparations were further purified by obtaining the flow-through fraction of 100-kDa molecular mass cutoff filters as described (21).

Human Brain Extracts—The Bioethics Committees and the Biosafety Committees of Mitsubishi Kagaku Institute of Life Sciences, Niigata University, and Kyoto University approved all experiments using human subjects. Freshly frozen brains obtained at autopsy were homogenized to 0.15 g/ml in an ice-cold extraction buffer (either 20 mM Tris-HCl, pH 7.6, 137 mM NaCl, or F12 buffer without L-glutamine and phenol red, containing 1 mM EDTA, 1 mg/ml pepstatin, and complete protease inhibitor mixture (Roche Diagnostics)) using a Potter Teflon/glass homogenizer. Soluble fractions were collected as the supernatant following centrifugation at 104,300 × *g* (TLA100.4) at 4 °C for 1 h. SDS-extractable insoluble fractions were obtained from the pellet by homogenizing in 2% (w/v) SDS and by 1-h gentle shaking at 37 °C, followed by centrifugation for 1 h at 10 °C. Formic acid-extractable fractions were obtained by homogenizing the SDS pellet in 70% formic acid, followed by centrifugation for 1 h. Approximate protein recoveries were 10% for soluble fractions and 90% for insoluble fractions. The possibility of artificial generation of ASPD-like structures from Aβ-(1–42) monomers or of destruction of ASPD-like structures during the extraction procedures was excluded (data not shown). More details are given in the supplemental Experimental Procedures.

Immunoprecipitations (IP)—To remove other assemblies (<100 kDa), soluble extracts from AD or NCI brains were concentrated using 100-kDa molecular mass cutoff filters (Millipore). This process was repeated until we obtained AD-derived 100-kDa retentates that contained native ASPDs at ~10–20 μM; this was verified by dot blotting using rpASD1. IPs were performed using an immunocapturing kit 100 MB-IAC Prot G (Bruker Daltonics), according to the manufacturer's instructions, except that 3% (w/v) bovine serum albumin (Sigma A7030) was used to suppress nonspecific binding. Monoclonal ASD antibodies (haASD1 or mASD3) were used for the immunoisolation because of their high affinity for ASPDs. Captured proteins were eluted using Gentle Elution buffer (Pierce),

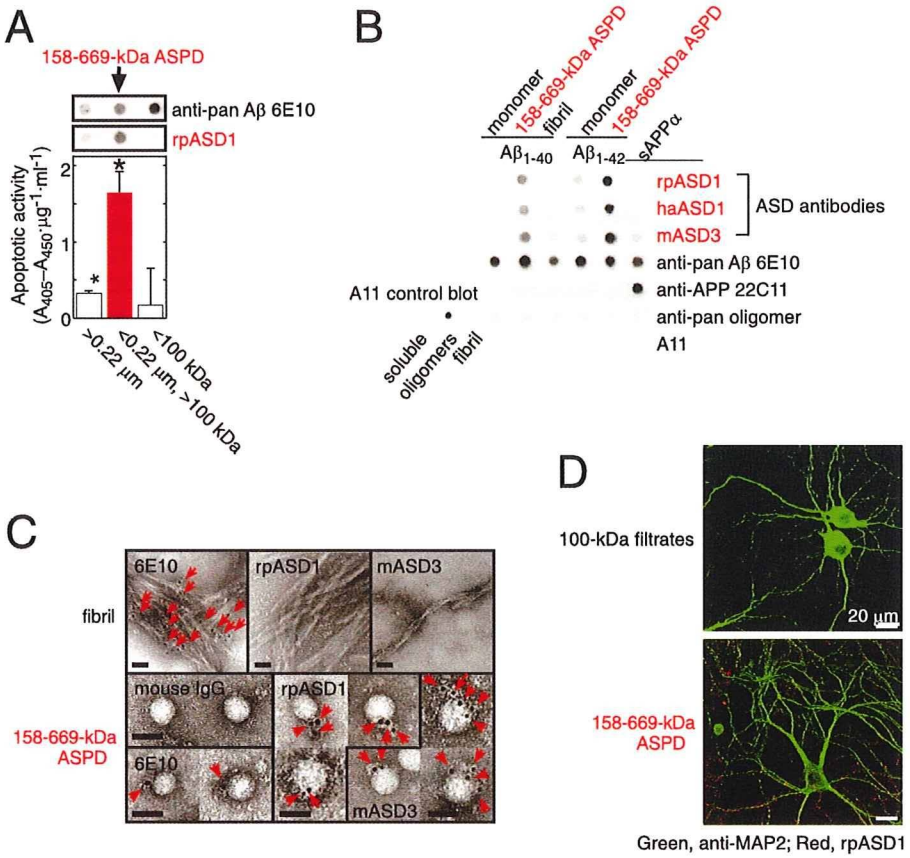

FIGURE 1. **Characterization of ASD antibodies.** *A,* evaluation of two-step filtered fractions (0.22-μm retentates, the 158–669-kDa ASPDs, and 100-kDa filtrates; see Scheme 1 under "Experimental Procedures") by dot blotting using rpASD1 and 6E10 (*upper panel*) and by toxicity assays using rat primary septal cultures (*lower panel*; mean ± S.D.; Games-Howell post hoc test, *, $p < 0.001$, $n = 6$). *B,* dot blotting of Aβ and APP (5 ng/dot). Synthetic ASPDs were prepared *in vitro* either from Aβ-(1–40) or Aβ-(1–42) as described (7). Purified 158–669-kDa ASPD fraction was recovered in 100-kDa retentates as in *A*. Unlike anti-APP-(66–81) (22C11), anti-Aβ-(1–16) (6E10), or A11 antibody, ASD antibodies selectively detected synthetic ASPDs and the 158–669-kDa ASPDs. The control blot membrane for A11 was provided by Invitrogen (supplemental Experimental Procedures). *C,* immuno-TEM analysis. *Arrows* show the secondary antibody-conjugated immunogold. 6E10 detected the 158–669-kDa ASPDs weakly, probably because of its low affinity for synthetic ASPDs. rpASD1 and mASD3 showed little reactivity to fibrils but clearly detected the 158–669-kDa ASPDs. *Bar,* 20 nm. *D,* rpASD1 detected intense signals in 27-DIV mature rat hippocampal neurons treated with the 158–669-kDa ASPDs (in *A*) for 30 min but did not detect signals in those treated with the 100-kDa filtrates containing monomers and Aβ-(1–42) assemblies with mass <100 kDa. Z-stack images are shown (supplemental Experimental Procedures).

because ASPDs retained their structure and toxicity (~100%) after a 60-min exposure to this buffer. The amount of native ASPDs in eluates was immediately examined by dot blotting with polyclonal rpASD1, a suitable antibody for dot blot analysis. Details are given in supplemental Experimental Procedures.

Other Methods—Preparation and screening of ASD antibodies, dot blotting, Western blotting, TEM and immuno-TEM examinations, surface plasmon resonance by Biacore and competitive enzyme-linked immunosorbent assay experiments, pathologic examinations of human brains, *Tg2576* mice experiments, toxicity assays, immunocytochemistry, human neuronal cells, and monkey neural progenitors and neurons, as well as statistics, are described in supplemental Experimental Procedures.

RESULTS

Production and Characterization of ASPD-specific Antibodies—To isolate native ASPDs from AD patients, we raised antibodies against ASPDs in 6 rabbits, 43 mice, and 10 hamsters. As an immunogen, synthetic ASPDs were prepared *in vitro* from 50 μM solutions of Aβ-(1–42) by slowly rotating the solutions for 14 h (38); they included spherical Aβ assemblies of 5–25 nm (>85% of them were 10–15-nm spheres). IgG-class antibodies were purified and named "ASD antibodies," with prefixes indicating the source (rabbit polyclonal as rpASD1; hamster monoclonal as haASD1; mouse monoclonal as mASD3).

We examined the reactivity of ASD antibodies against the most toxic synthetic ASPD fraction separated as follows. Because the mass of the most toxic 10–15-nm ASPDs is almost equal to that of 158-kDa aldolase but does not exceed that of 669-kDa thyroglobulin in sedimentation analysis (38), synthetic ASPDs were further size-separated by means of two-step filtrations (see Scheme 1 under "Experimental Procedures") to concentrate the most toxic 158–669-kDa ASPDs in fraction b, the fraction that passed through 0.22-μm filters but was retained on 100-kDa molecular mass cutoff filters. As expected, 158–669-kDa ASPDs recovered in fraction b included 10–15-nm spheres, as determined by TEM observation (data not shown), and were confirmed to be the most toxic species in toxicity assays (Fig. 1*A*).

Importantly, rpASD1 specifically detected the 158–669-kDa ASPDs in fraction b in dot blotting but had little or no cross-reactivity to fraction a 0.22-μm retentates or fraction c 100-kDa filtrates containing monomers and 5–6-nm particles, which are strongly detected by anti-pan Aβ 6E10 antibody (Fig. 1*A*). We also confirmed that rpASD1 did not cross-react with ADDLs (supplemental Fig. S1*A*). These results indicated that rpASD1 recognizes an epitope that is associated with the most toxic ASPDs but not with ADDLs.

We further characterized rpASD1 and the other ASD antibodies using the most toxic 158–669-kDa ASPDs. As shown in Fig. 1*B*, all ASD antibodies detected primarily the 158–669-kDa ASPDs (prepared from either Aβ-(1–42) or Aβ-(1–40))

TABLE 1

Summary of characters of ASD antibodies and anti-pan Aβ antibodies

The characters of newly established anti-ASPD antibodies (upper three rows) and previously reported anti-pan Aβ antibodies (lower two rows) are summarized. The original epitope mapping data are shown in supplemental Fig. S1*B*; see Fig. 1*A* and supplemental Fig. S3*A* for dot blots and supplemental Table S2 for K_d values determined by Scatchard analysis of enzyme-linked immunosorbent assay data; see Fig. 1*C* (except haASD1) for immuno-TEM and supplemental Fig. S5*A* for toxicity blockade.

Antibody	Preference among Aβ types in dot blotting	K_d for ASPDs	Epitope map	Response to APP in dot blotting	Response to fibrils in immuno-TEM	Blockade of ASPD toxicity
		nM				
rpASD1	ASPD	0.005	Several regions[a]	−	−	+
mASD3	ASPD	0.003	Several regions[a]	±	−	+
haASD1	ASPD	0.0005	Could not be determined[b]	−	−	−
6E10	All types	0.2	Aβ5–9[c]	+	+	−
82E1	All types	ND[d]	Aβ1–5[c]	−	ND	−

[a] The binding of these antibodies to synthetic-ASPDs was most strongly inhibited by N-terminal pentapeptides of Aβ. In addition, the binding was also inhibited by specific sets of non-N-terminal pentapeptides. The data suggest that different Aβ regions exist in close proximity to form the ASPD-specific epitope.
[b] The binding of haASD1 to synthetic-ASPDs was not inhibited by the addition of any pentapeptide, suggesting that haASD1 recognizes a nonlinear epitope formed by noncontiguous Aβ regions.
[c] For 6E10 and 82E1, which did not discriminate ASPDs from other types of Aβ, complete inhibition was attained with a single pentapeptide in each case.
[d] ND means not determined.

but had very low or no cross-reactivity to sAPPα (human secreted form of APP), Aβ monomers, or Aβ fibrils, whereas 6E10 equally detected all these Aβ species and sAPPα (Fig. 1*B*). Consistent with this, ASD antibodies detected 10–15-nm spheres in the 158–669-kDa ASPDs but did not react with fibrils as observed with immuno-TEM under mild fixation conditions (Fig. 1*C*). In accordance with their ASPD preference in dot blots and immuno-TEM, the ASD antibodies showed the highest affinity for the 158–669-kDa ASPDs (K_d 10^{-12}–10^{-13} M; Table 1), rather than for Aβ monomers, fibrils, or sAPPα (supplemental Table S2). These results demonstrated ASPD specificity of all the ASD antibodies. As described above, A11 antibody is a pan-oligomer polyclonal antibody that recognizes epitopes associated with an oligomer state (18, 19, 22). To our surprise, this anti-pan oligomer A11 antibody failed to detect the 158–669-kDa ASPDs (Fig. 1*B*). These results strongly suggested that epitopes recognized by the ASD antibodies are associated with the tertiary structure of ASPDs, which differs from that of A11-positive oligomers, such as Aβ*56 and AβOs, and from that of fibrils. To further elucidate the epitope specificity, we performed epitope mapping by means of competitive enzyme-linked immunosorbent assay using a series of pentapeptides covering the entire Aβ-(1–42) sequence. As summarized in Table 1, no single pentapeptide could compete out binding of the ASD antibodies to the 158–669-kDa ASPDs, suggesting that different Aβ regions exist in close proximity within ASPDs to form ASPD tertiary structure-dependent epitopes that are not present in a single Aβ monomer (supplemental Fig. S1*B*). The ASD antibodies produced only weak or no bands in Western blots under denaturing conditions (data not shown), as would be expected from the fact that they recognize ASPD tertiary structure. We finally examined whether the ASD antibodies are available for detecting ASPDs bound to mature neurons, because we have previously shown that synthetic ASPDs directly induce neuronal cell death, possibly by binding to neuronal cell surfaces (38). As shown in Fig. 1*D*, the ASD antibodies clearly detected synthetic ASPDs bound on mature rat hippocampal neurons (see "Experimental Procedures") when the neurons were briefly treated with the 158–669-kDa ASPDs and fixed under mild conditions, but they did not label neurons treated with the 100-kDa filtrates, which contained monomers and 5–6-nm particles of less than 100 kDa. The characteristics of the antibodies are summarized in Table 1. All of these results demonstrate that the ASD antibodies recognize epitopes that are specific to the surface tertiary structure of ASPDs, which differ from that of ADDLs, A11-positive prefibrillar oligomers, and fibrils.

ASPD-specific Antibody-stained AD Brain—To elucidate whether synthetic ASPD-like assemblies are present *in vivo*, brain sections of patients with clinico-pathologically confirmed AD (41) (n = 10; age 80.4 ± 9.2 years, brain weight 964 ± 82 g, disease duration 10.1 ± 5.5 years) and those of NCI people (n = 7; age 71.3 ± 15.2 years, brain weight 1226 ± 96 g) were immunostained with ASD antibodies. The reactivity of the ASD antibodies in AD patients was strongly associated with brain regions where prominent neurodegeneration had occurred (*e.g.* temporal cortex, frontal cortex, and hippocampus) (Fig. 2*A* and supplemental Fig. S2) but was rarely observed in NCI brains (data not shown). This immunoreactivity in AD brains was associated mainly with plaques and occasionally with neurites and some microvessels and was eliminated by prior treatment of the ASD antibodies with the 158–669-kDa ASPDs (data not shown).

We next compared the reactivity to plaques under various conditions between the ASD antibodies and anti-pan Aβ antibodies, the most widely used antibodies for detecting fibrils in plaques. Although anti-pan Aβ antibodies labeled plaques only in formalin-fixed paraffin sections after pretreatments such as microwaving or formic acid, ASD antibody-specific reactivity was observed most strongly in cryosections and more weakly in formalin-fixed paraffin sections with or without pretreatments (except that haASD1 is available only for cryosections) (Fig. 2*A*). This difference in immunoreactivity to plaques suggested that anti-pan Aβ antibodies and ASD antibodies detect different structures in plaques; anti-pan Aβ antibodies detect fibrils when buried epitopes are exposed by protein-denaturing treatments, whereas ASD antibodies are considered to detect tertiary structure-dependent epitopes on putative human ASPD counterparts under conditions where the native structure of proteins is preserved. To confirm this, we performed biochemical fractionation of AD brains and examined whether these antibodies reacted with insoluble or soluble fractions. Consistent with previous data that fibrils include an insoluble core of plaques (42), anti-pan Aβ antibodies reacted mainly (>85%)

Isolation of Toxic High Mass Aβ Assembly from AD Patients

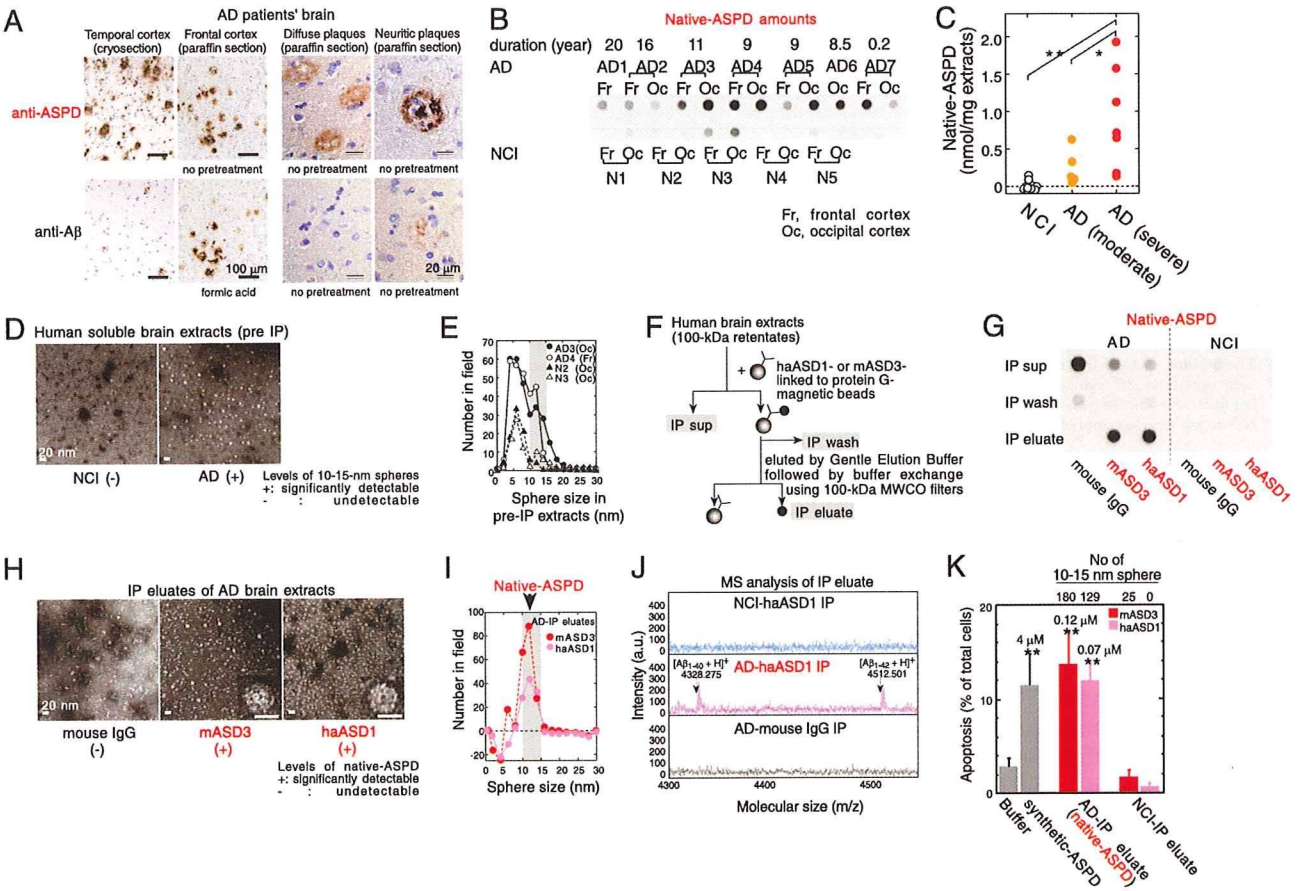

FIGURE 2. **Isolation of native ASPDs.** *A*, AD brains were stained with rpASD1 (5 μg/ml) or anti-Aβ1–42 C-terminal antibody (0.5 μg/ml; 2 μg/ml for cryosections). *B* and *C*, dot blotting of 100-kDa retentates (>100 kDa) of AD or NCI brain extracts (1 μg of soluble extracts/dot) using rpASD1 (Scheffé post hoc test; **, $p = 0.0011$; *, $p = 0.0388$). *Fr*, frontal cortex; *Oc*, occipital cortex. *D* and *E*, TEM images (*D*) and particle analysis of 100-kDa retentates ($n = 3$; 10 randomly selected fields) (*E*). *F* and *G*, method for immunoprecipitation (*IP*) (*F*) and dot blotting (using rpASD1) of IP supernatants (*sup*), wash, and eluate fractions. IPs were performed using haASD1, mASD3, or mouse IgG (*G*). *H* and *I*, TEM images (*inset*, *bar*, 10 nm) (*H*) and particle analysis of IP eluates ($n = 3$; 15 randomly selected fields, background (a small amount of spheres <10 nm contained in eluate with buffers)-subtracted data are shown) (*I*). *J*, representative MALDI-TOF/MS data. Aβ-(1–40) and Aβ-(1–42) were detected only in native ASPDs at theoretical monoisotopic mass values (($[A\beta\text{-}(1\text{–}40) + H]^+$, 4328 Da; $[A\beta\text{-}(1\text{–}42) + H]^+$, 4512 Da) as observed in synthetic Aβ peptides. *K*, toxicity of isolated native ASPDs toward primary rat septal neurons (mean ± S.D.; Scheffé post hoc test, **, $p < 0.0001$, compared with buffer, $n > 8$) correlated with the 10–15-nm sphere number determined as in *I*. Neurons treated with NCI-IP eluates showed only background levels of apoptosis similar to those of neurons treated with buffers. *Inset*, synthetic or native ASPD amounts in Aβ monomer concentrations.

with insoluble fractions of AD brains extracted with SDS or formic acid (supplemental Fig. S3*A*). Furthermore, this insoluble fraction produced broad smears in Western blots of Aβ, as is usually observed with fibrils (42) (supplemental Fig. S3*B*). In contrast, the ASD antibodies reacted only with soluble fractions of AD brains (supplemental Fig. S3*A*) in which the human ASPD counterpart was actually present, as described below (see under "Isolation of Native ASPD from Brains of AD Patients"). These results collectively indicate that the ASD antibodies detect a human ASPD counterpart, namely native ASPD, associated with plaques and neurites in AD brains. In subsequent work, we used monoclonal mASD3 and haASD1 for isolating ASPDs, because of their high affinity, and polyclonal rpASD1 for detecting ASPDs (except Fig. 3*A*; see also "Immunoprecipitations" under "Experimental Procedures").

Isolation of Native ASPD from Brains of AD Patients—The tissue fractionation study revealed that native ASPDs are recovered in soluble fractions of AD brains. To investigate the amount of native ASPD, we prepared soluble fractions of AD brains ($n = 7$; age 85.6 ± 3.1 years, brain weight 1025 ± 104 g) and NCI ($n = 5$; age 72.6 ± 9.5 years, brain weight 1236 ± 64 g) by means of a nondenaturing procedure using solutions of physiologic ionic strength and pH without detergents. We then obtained 100-kDa retentates of the soluble fractions to concentrate native ASPDs (larger than 100 kDa) and to eliminate other Aβ assemblies smaller than 100 kDa (as performed in Fig. 1*A*). The 100-kDa retentates of AD brains thus obtained had high levels of rpASD1-reactive substances, but those of NCI brains had very low or negligible reactivity (Fig. 2*B*). Consistent with the above data, much higher numbers of spheres sized 10–15 nm were present in 100-kDa retentates of AD patients than in those of NCI (Fig. 2, *D* and *E*). These results suggest that rpASD1-reactive 10–15-nm spheres in 100-kDa retentates of AD are native ASPD candidates. We then immunoisolated native ASPDs (Fig. 2*F*) from large amounts of AD-derived 100-kDa retentates using two monoclonal antibodies, haASD1 and mASD3 (Fig. 2, *G–J*). These antibodies were chosen for their extremely high affinity for ASPD ($K_d < 10^{-12}$ M) and for their

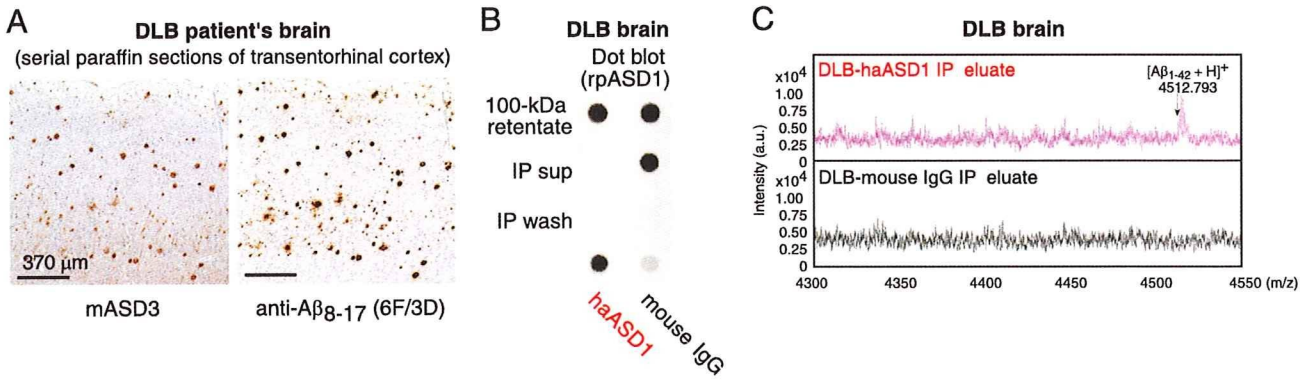

FIGURE 3. **Native ASPDs exist in DLB brains.** *A*, immunostaining using mASD3 (2.5 μg/ml) and anti-Aβ8–17 (pretreated with formic acid; 1:100; DAKO). *B*, IP was performed with haASD1 or mouse IgG as in Fig. 2*F* using 100-kDa retentates (4 μg of soluble brain extracts/IP). Dot blotting (0.04 μg/ml rpASD1) of 100-kDa retentates (2 μg of soluble brain extracts/dot), IP supernatants (*sup*), wash, and eluate is shown. *C*, representative MALDI-TOF/MS data.

recognition of different epitopes (Table 1). Judging from the results of quantification of dot blots using rpASD1 (Fig. 2*G*), we obtained about 43 pmol of native ASPDs (expressed as Aβ monomer concentration) from 1 g of AD brain tissues ($n = 6$). The rpASD1 reactivity in the IP eluates was considered to be mostly due to the 10–15-nm spheres, because the number of spheres counted by TEM (Fig. 2*H*) (1.0×10^{10} 10–15-nm sphere/μl estimated from the number of spheres in Fig. 2*K*, $n = 6$) was very similar to the amount of rpASD1-reactive ASPD obtained from dot blots (1.1×10^{10} native ASPD/μl based on the ASPD concentration in Fig. 2*K*, $n = 8$). This means that rpASD1-reactive 10–15-nm spheres were selectively isolated by a combination of 100-kDa retention and IP. Indeed, as shown by the TEM data (Fig. 2*H*), the non-ASPD small-sized spheres (<10 nm) that had been present in large amounts in 100-kDa retentates of AD and NCI were largely eliminated by the IP procedure (compare Fig. 2, *I* with *E*). Accordingly, we successfully isolated native ASPDs, consisting of 10–15-nm spheres (>95%; Fig. 2, *H* and *I*), from 100-kDa retentates of AD. In contrast, native ASPD-like assemblies were scarcely detected in IP eluates from 100-kDa retentates of NCI (Fig. 2, *G* and *K*). We next examined whether native ASPDs consisted of Aβ. Mass spectrometric analysis showed that singly charged ions corresponding to Aβ-(1–42) and Aβ-(1–40) were detected in native ASPDs (Fig. 2*J*). These results collectively demonstrate that 10–15-nm spherical Aβ assemblies isolated from AD brains are native ASPDs. Notably, anti-pan Aβ 6E10 could not immunoisolate native ASPDs (data not shown), probably because of its weak affinity for ASPDs ($K_d \approx 10^{-9}$ M) compared with ASD antibodies ($K_d < 10^{-12}$ M) (Table 1). We also confirmed that anti-pan oligomer A11 antibody failed to detect native ASPDs (supplemental Fig. S4).

Having isolated native ASPDs selectively from human AD brains, we next examined whether they elicited neurodegeneration of rat primary neuronal cells. Surprisingly, AD-derived native ASPDs were even more toxic than synthetic ASPDs (Fig. 2*K*). These results collectively demonstrate that we have newly isolated A11-negative, high mass assemblies that cause neuronal cell death and that differ in mass and surface tertiary structure from other reported nonfibrillar Aβ assemblies.

Native ASPD Amount Correlates with the Pathologic Severity of AD—We next examined whether the amount of native ASPD correlated with the pathologic severity of AD brains. Larger amounts of native ASPD were present in AD patients with severe pathology (diagnosed "C" according to the CERAD criteria (43)) than in AD patients with moderate pathology (diagnosed "B") (Fig. 2*C*). Furthermore, in AD patients with severe pathology, significantly higher amounts of native ASPD were detected in the frontal or temporal cortices (7.2 ± 1.5 nmol/g brain tissue, $n = 3$, Scheffé post hoc test $p = 0.0012$) than in the cerebellum (0.14 ± 0.1 nmol/g brain tissue). The result is consistent with previous findings that the cerebellum in AD is pathologically less affected (44, 45).

The above observations suggest the involvement of native ASPDs in neurodegeneration of AD brains. We therefore examined brains of patients suffering from DLB, the second most frequent cause of cognitive decline associated with neurodegeneration in the elderly (46, 47), because the majority of DLB brains have been shown to have AD-type pathology, including plaques (46–48). Interestingly, native ASPDs were also isolated from DLB brains (Fig. 3, *A–C*).

AD-derived Native ASPDs Cause Severe Degeneration of Human Neuronal Cells—To further elucidate the relationship between neuronal loss and native ASPDs, we first examined whether native ASPDs induce degeneration of human mature neuronal cells. Because studies using human primary neurons are problematic for ethical and practical reasons, cells with neuronal properties were induced from human bone marrow stromal cells (MSCs) (49). Initially, postmitotic neuronal cells were induced from human MSCs (>95% were neuron-specific MAP2ab-positive cells without glia) (49). Treatment of these cells with glial cell line-derived neurotrophic factor promoted their maturation into functional neuronal cells (49). We found that a 2-day treatment of the human MSC-derived functional neuronal cells with isolated native ASPDs caused severe degeneration, whereas IP eluates from NCI brains had no effect (Fig. 4*A*). In addition, pretreatment with mASD3 antibody (100 μg/ml) significantly blocked this toxicity (Fig. 4*A*), as observed in the case of the 158–669-kDa ASPDs (supplemental Fig. S5*A*), dem-

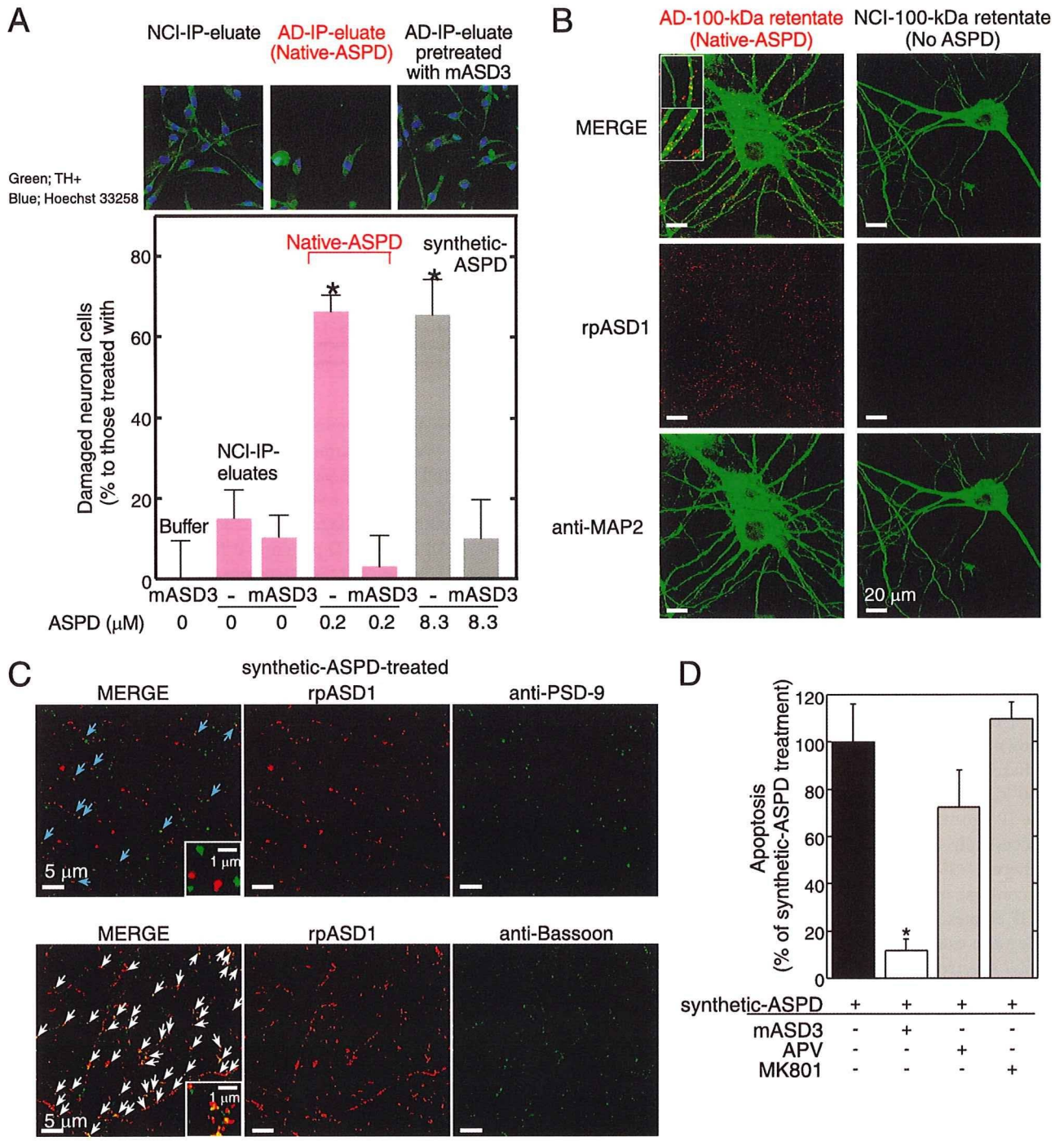

FIGURE 4. **Characterization of native and synthetic ASPD-induced toxicity.** *A,* IP was performed using haASD1 as in Fig. 2*F*. Human neuronal cells were treated for 2 days with AD or NCI-IP eluates, with or without 2-h mASD3 (100 μg/ml) pretreatment. Nondamaged cells were counted after tyrosine hydroxylase (*TH*+) and Hoechst 33258 staining. The ratio of damaged cells to neuronal cells treated with buffer alone (mean ± S.D.) is shown (Scheffé post hoc test; *, $p < 0.0001$, $n = 5$). Neuronal cells treated with mASD3 alone or NCI-IP eluates showed only background levels of damaged cells similar to those in the case of cells treated with buffer. *B* and *C*, mature rat hippocampal neurons (24 DIV in *B* and 19 DIV in *C*) were incubated for 30 min either with 100-kDa retentates of AD (containing 0.8 μM native ASPDs) or NCI (no native ASPD detected) brain extracts in *B* or with 0.5 μM 158–669-kDa ASPDs (prepared from Aβ-(1–42); see Fig. 1*A*) in *C*. Bound ASPDs were detected by rpASD1, as in Fig. 1*D*. Punctate labeling was found primarily on neurites and surrounding cell bodies of neurons treated with native or synthetic ASPDs, but it was hardly detectable in neurons treated with the NCI retentates. A representative high power view is shown in the *inset* (*B*; *bar*, 5 μm). Neurons were co-stained with an antibody against anti-MAP2 in *B*, against a postsynaptic marker PSD-95 in *C* (*upper panels*), or against a presynaptic marker bassoon in *C* (*lower panels*). Z-stack images are shown (except *lower panels* in *C*) as in Fig. 1*D*. Bound ASPDs did not co-localize with PSD-95 but were concentrated with bassoon (*white arrows* in *C*), although they were occasionally localized in close proximity to PSD-95 (*blue arrows* in *C*). *D*, mature rat hippocampal neurons (21 DIV) were treated with 1 μM 158–669-kDa ASPDs for 2 days, with or without pretreatment (100 μg/ml mASD3 for 2 h; competitive (APV) or uncompetitive (MK801) NMDA-R antagonists (10 μM) for 30 min). Data represent mean ± S.D. (Scheffé post hoc test; *, $p = 0.0039$, compared with synthetic ASPDs; synthetic ASPDs, $n = 7$; synthetic ASPDs + APV or MK801, $n = 5$; synthetic ASPDs + mASD3, $n = 4$).

onstrating that the observed neuronal cell death was caused by native ASPDs.

We then examined whether native ASPDs bind mature rat hippocampal neurons, as is observed in the case of synthetic ASPDs (Fig. 1*D* and supplemental Fig. S5*B*). Binding of AD-derived native ASPDs to 24-DIV mature rat hippocampal neurons was detected with rpASD1 most intensely in neurites and also to some extent in cell bodies (Fig. 4*B*). These results suggest that, despite the difference in dose dependence of neurotoxicity (Figs. 2*K* and 4*A*), native and synthetic ASPDs share essentially the same mechanism of neurotoxicity, *i.e.* they have the same surface tertiary structure that is responsible for exerting the toxicity. We speculate that the apparent difference in dose dependence might be attributed to differences in molecular compositions, but testing this idea will require further analyses using large amounts of isolated native ASPDs.

Mode of Native ASPD Neurotoxicity Is Different from That of Other Reported Aβ Assemblies—The above results (Fig. 4, *A* and *B*) show that native ASPDs cause neuronal cell death, possibly by binding to neuronal cell surfaces. We therefore examined ASPD-binding sites on mature neurons to elucidate the molecular basis of native ASPD neurotoxicity. As shown in the high power images in Fig. 4*B* (*inset*), bound native ASPDs appeared to protrude from the MAP2 staining of dendrites. Essentially the same results were obtained with the binding of synthetic ASPDs (supplemental Fig. S5*B* (*inset*)). Because of the limited availability of native ASPDs, we employed synthetic ASPDs for further analysis, as synthetic and native ASPDs share essential properties. Consistent with the above observation, the binding of synthetic ASPDs did not co-localize with a postsynaptic marker, PSD-95 (Fig. 4*C*, *upper panel*), although it was occasionally detected in close proximity to PSD-95 (*blue arrows* in *C*). Instead, ASPD-binding sites appeared to be concentrated at presynaptic sites stained by the antibody against a presynaptic marker, bassoon (*white arrows* in Fig. 4*C*, *lower panel*).

Although previous studies using cell or slice culture systems have found that Aβ assemblies such as dimers, ADDLs and AβOs bind postsynapses and depend on postsynaptic signaling mechanisms for exerting synaptotoxicity (23), the presynaptic binding of ASPDs apparent in Fig. 4*B* suggests that ASPD neurotoxicity would not require postsynaptic signaling mechanisms such as the *N*-methyl-D-aspartate glutamate receptor (NMDA-R) pathway. Indeed, neither a competitive (APV) nor an uncompetitive (MK801) NMDA-R antagonist inhibited synthetic ASPD-induced neurodegeneration (Fig. 4*D*). As noted above, native and synthetic ASPDs share the common surface tertiary structure responsible for exerting the toxicity. Therefore, the findings obtained with synthetic ASPDs (Fig. 4, *C* and *D*) strongly suggest that native ASPDs cause neuronal cell death through presynaptic target(s) on mature neurons. Furthermore, these observations are consistent with the findings indicating that native ASPDs have a distinct surface tertiary structure from other reported Aβ assemblies and support the hypothesis that native ASPDs have a different target(s) from other Aβ assemblies.

DISCUSSION

Aβ assemblies are considered to acquire surface tertiary structures that are not present in physiologic Aβ monomers and that induce synaptic impairment and neuronal loss through interactions with neuronal cells. Therefore, as recently suggested (12), it is reasonable to classify seemingly different Aβ assemblies in terms of their immunoreactivity to antibodies that recognize particular surface tertiary structure. Because the surface tertiary structure mediates the binding of Aβ assemblies to their target(s) and is therefore responsible for exerting the toxic effects, Aβ assemblies having distinct surface tertiary structures are likely to have distinct mechanisms of neurotoxicity and may contribute differently to the disease development. Here we have demonstrated the existence of patient-derived native ASPDs by selectively immunoisolating them from AD and DLB brains (Figs. 2 and 3) using ASPD tertiary structure-dependent antibodies (Fig. 1 and Table 1). The native ASPDs (>100 kDa) thus obtained are larger in mass than AD-derived Aβ dimers and other reported assemblies such as 12-mers (53~60 kDa; ADDLs, globulomer, Aβ*56) or AβOs (~90 kDa) (supplemental Table S1). More importantly, native ASPDs are considered to have a distinct surface tertiary structure from those other assemblies because they differ in immunospecificity, as illustrated by the fact that ASPD tertiary structure-dependent antibodies showed minimal reactivity with the 100-kDa filtrate containing monomers and dimers (Fig. 1*A*) or with ADDLs (supplemental Fig. S1*A*) (16) in dot blots. Additionally, anti-pan oligomer A11 antibody (22) recognized AβOs but not synthetic ASPDs (Fig. 1*B*) or native ASPDs (supplemental Fig. S4). Finally, anti-Aβ N-terminal antibodies such as 82E1 blocked the synaptotoxicity of AD-derived dimers (30) but failed to block synthetic ASPD-induced neurodegeneration (supplemental Fig. S5*A*). These results all indicate a difference in the surface tertiary structure between these assemblies and ASPDs.

As for the cellular basis of the Aβ-induced synaptic changes, previous studies have suggested the involvement of postsynaptic signaling mechanisms (23). For example, the binding of ADDLs and AβOs has been reported to co-localize with PSD-95 (19, 23). As expected from the postsynaptic locale of their binding, ADDLs bind close to or at NMDA-R (23), and NMDA-R antagonists inhibit ADDL-induced dendritic changes (23), reactive oxygen species formation (50), and insulin receptor impairment (51). NMDA-R antagonists have also been reported to inhibit Aβ dimer-induced synaptic loss (24, 30). Interestingly, cellular prion protein, which interacts with NMDA-R (52), has recently been reported to serve as a high affinity postsynaptic receptor mediating ADDL-induced synaptic dysfunction (53). Taken together, these studies are consistent with the idea that Aβ dimers, ADDLs, and AβOs perturb postsynaptic transmission (19, 23, 30).

We found that, unlike the above Aβ assemblies, ASPDs bind presynaptic target(s) on neurons to induce neurodegeneration (Fig. 4, *A–C*). This may be reasonable in view of the distinct ASPD surface tertiary structure. Although the actual targets of native ASPDs remain to be elucidated, native ASPDs seem to affect mature neuron-specific molecules or cellular pathways,

as synthetic ASPD-induced neurotoxicity appeared to be confined to neurons, being especially active toward mature neurons, but sparing non-neuronal cells and immature neurons (supplemental Fig. S6, *A–C*). Together, the findings indicate that native ASPDs are patient-derived, A11-negative, high mass Aβ assemblies with a distinct toxic surface that binds presynaptic target(s) on mature neurons, leading to neuronal loss (supplemental Table S1). Although further studies are required to reveal how native ASPDs exert neurotoxicity in the brains of patients with AD, our findings indicate for the first time that presynaptic signaling mechanisms may play a critical role in Aβ-induced neurodegeneration in AD.

Recent *in vivo* as well as *in vitro* studies support the toxicity of nonfibrillar Aβ assemblies and their possible causative roles in the neuropathology of AD (54–56), which is consistent with the dissociation between fibril load and cognitive decline in patients with AD (32, 57, 58). Thus, Aβ assemblies other than fibrils have been considered to be the preferred therapeutic targets for AD (54). However, the nature of the Aβ species and the oligomer state responsible for the pathogenesis remain controversial because of the heterogeneity of Aβ assemblies in terms of Aβ species and oligomer size. It is also unknown how Aβ monomers assemble into oligomers in living human brains. Nevertheless, previous *in vitro* studies have shown that Aβ monomers develop into a variety of assemblies that might represent distinct structural variants (10–13). These studies suggest that assembly may not be a linear process but may be the result of a series of multiple processes involving intermediates from side paths. Taking all the results together, it seems reasonable to assume that the brains of patients with AD contain distinct types of Aβ assemblies with different surface tertiary structures that may play different roles in AD development. Therefore, identification and characterization of all types of Aβ assemblies actually present in brains from humans with AD will be important for understanding the molecular mechanisms underlying the AD progression from the initial step to the symptomatic phase and for the development of therapies based on this understanding. Fractionation studies using oligomer tertiary structure-dependent antibodies as shown here will help to elucidate the assembly process and to determine the Aβ assembly state causing the pathogenesis. We have isolated native ASPDs that cause degeneration of mature human neuronal cells *in vitro* (Fig. 4*A*) and have shown that the amount of native ASPD is correlated with the pathologic severity of clinically proven AD cases (Fig. 2*C*).

These findings suggest that native ASPDs might be a candidate for Aβ assemblies that directly cause neuronal loss in the brains of humans with AD. However, it remains to be elucidated whether or not ASPDs play a particular role in the onset or early stage of disease development. Braak and coworkers (59) have compared the expansion of Aβ pathology in whole brain regions between AD cases and nondemented cases with or without Aβ-related pathology. They found that patients with clinically proven AD exhibit late Aβ stages, although the nondemented cases with AD-related pathology show early Aβ stages. Their findings suggest that AD brains develop pathologic Aβ deposition before clinical symptoms become apparent, and this may start much earlier in nondemented patients with AD-related Aβ pathology. Quantitative studies, with the assistance of clinicians, on the brains of people in different Aβ stages, including nondemented people with AD-related Aβ pathology, will be helpful to elucidate if ASPDs play a role in neuronal loss in AD from the early stage of disease development.

Analyses on brains of APP-transgenic mice with or without neuronal loss would also help to elucidate the relationship between ASPDs and neuronal loss. Although the strain does not show neuronal loss, we examined *Tg2576* mice, the most widely used AD-model mice carrying the human Swedish APP mutant (60), by means of immunohistochemistry and IP. ASPD-like assemblies were only minimally detected in the cerebral cortex of *Tg2576* mice (supplemental Fig. S7, *A* and *B*);: they were not detected up to 14 months and only a very small amount (~0.01 nmol/mg extracts) was detected at 23 months. As previously reported (18, 61), other Aβ assemblies such as dimers and Aβ*56 were increased in *Tg2576* mice, and total Aβ reached levels comparable with those in human AD (supplemental Fig. S7*C*). With respect to mice with neuronal loss, in addition to certain APP transgenic mice (28, 29), there is a growing number of other AD-model mice, which have been produced by combining APP mutations with either presenilin-1 mutations (62, 63), Tau protein mutations (64), or nitric-oxide synthase knock-out (65). It should be noted that the mouse is not a perfect model of human AD, but these mice are considered to more closely resemble what occurs in the human brains. Therefore, further analysis to examine whether ASPD-like assemblies are present in these mice, which do show massive neuronal loss, will contribute to establish the relationship between neuronal loss and ASPDs.

In addition to the above, we are currently seeking to establish a direct link between native ASPDs and neuronal loss in brains from humans with AD by searching for the toxic target(s) of ASPDs on mature neurons. The identification of native ASPDs and availability of the toxicity-neutralizing antibodies should facilitate a mechanistic understanding of the cellular basis of neuronal cell loss in AD, as well as the development of therapies based on this understanding.

Acknowledgments—We thank Drs. George R. Martin, Takaomi C. Saido, Sangram S. Sisodia, R. Yu, Y. Fukazawa, D. Masui, M. Hoshino, H. Hara, and A. Sakai, for critical discussions; Dr. Charles G. Glabe for providing control blots for A11 antibody through Invitrogen; and Drs. T. Nirasawa, S. Horie, H. Kinoshita, S. Miyama, Y. Ogawa, and N. Takino for technical assistance.

REFERENCES

1. Ross, C. A., and Poirier, M. A. (2005) *Nat. Rev. Mol. Cell Biol.* **6,** 891–898
2. Selkoe, D. J. (1991) *Neuron* **6,** 487–498
3. Lansbury, P. T., and Lashuel, H. A. (2006) *Nature* **443,** 774–779
4. Iwatsubo, T. (2007) *Neuropathology* **27,** 474–478
5. Soto, C., and Estrada, L. D. (2008) *Arch. Neurol.* **65,** 184–189
6. Chiti, F., and Dobson, C. M. (2009) *Nat. Chem. Biol.* **5,** 15–22
7. Hardy, J., and Selkoe, D. J. (2002) *Science* **297,** 353–356
8. Tanzi, R. E., and Bertram, L. (2005) *Cell* **120,** 545–555
9. Saido, T. C., and Iwata, N. (2006) *Neurosci. Res.* **54,** 235–253
10. Klein, W. L., Stine, W. B., Jr., and Teplow, D. B. (2004) *Neurobiol. Aging* **25,** 569–580